Including orbital fluctuations in the noise spectrum of autonomous circuits

International Journal of Microwave and Wireless Technologies, 2011, 3(1), 11–18.
doi:10.1017/S1759078710000826

Including orbital fluctuations in the noise spectrum of autonomous circuits

FABIO L. TRAVERSA[1] AND FABRIZIO BONANI[2]

We discuss the impact of orbital fluctuations on the noise spectrum of a free-running oscillator, exploiting a rigorous nonlinear perturbative analysis based on the Floquet theory, and providing evidence of its relevance for high-Q oscillators.

Keywords: Circuit simulation, Autononmous systems, Nonlinear oscillators, Oscillator noise

Received 11 August 2010; Revised 28 November 2010; first published online 18 January 2011

I. INTRODUCTION

Noise analysis in oscillators, despite its long history dating back to the 1930s [1–4], still receives a large interest, from both theoretical and practical standpoints, because of the inherent complexity of fluctuation analysis in autonomous systems, and of the significant impact of oscillator noise performance on communication receivers [5].

The widely accepted theory decomposes oscillator noise into time-reference fluctuations, which in analog applications are expressed in terms of *phase noise*, and into variations of the amplitude of the circuit working point: these give rise to the so-called *amplitude* or *orbital noise* contribution. Although the dominant component near to the oscillator frequency f_o (and to its harmonics kf_o, k integer) is phase noise, orbital fluctuations become the stronger contribution at large offset frequencies, and therefore in the presence of a strong adjacent channel they contribute to impair the dynamic range of the receiver [5].

The link between oscillator fluctuations and the circuit noise sources can be studied in several ways, with different degrees of complexity and, in turn, of accuracy. The two extrema are the purely linear perturbative analysis, and the full nonlinear treatment based on the derivation of a nonlinear partial differential equation having as unknown the probability density of the fluctuating state variables (i.e., the Fokker–Planck equation associated to the noisy oscillator dynamic equations). While the latter is of course a rigorous technique, its implementation is in general unpractical since very rarely a fully numerical integration can be avoided. On the other hand, in the linear perturbative approach the circuit variables are expressed as the sum of the noiseless oscillator value and of the noise-induced perturbation. Fluctuations are assumed of small amplitude, and the circuit is transformed into a linear time-varying system through linearization. This technique has been proved to provide an unphysical phase noise spectrum divergence for frequencies very close to the harmonics of the oscillating frequency, i.e., for vanishingly null offset (or sideband) frequency. Despite this limitation, however concentrated very near to f_o, linear perturbation is the most valuable tool in the hands of the circuit designer, at least for a first-order design, since quite often it allows for a fully analytical treatment.

The divergence issue has been overcome by the nonlinear perturbative analysis proposed in [6], where only the phase noise component was considered. We have recently extended this treatment by deriving a consistent statistical characterization of the entire correlation matrix, i.e., by considering not only the phase noise but rather including orbital fluctuations and their correlation with phase noise as well [7]. We discuss here some results of the application of this approach to a couple of examples, showing the effects of orbital noise and the impact of the oscillator Q factor on its magnitude.

II. A GLIMPSE ON THE MODELING APPROACH

We assume that the oscillator is a lumped circuit represented by the autonomous ordinary differential equation:

$$\frac{\mathrm{d}\mathbf{x}}{\mathrm{d}t} - \mathbf{f}(\mathbf{x}) = 0, \tag{1}$$

where $\mathbf{x}(t)$ is the circuit state vector of size n. Let us consider the non-trivial periodic solution (limit cycle, of period $T = 1/f_o$) $\mathbf{x}_S(t)$ for (1). We perturb (1) by adding the set $\xi(t)$ of white Gaussian noise sources, so that $\mathbf{z}(t)$ satisfies

$$\frac{\mathrm{d}\mathbf{z}}{\mathrm{d}t} - \mathbf{f}(\mathbf{z}) = \mathbf{B}(\mathbf{z})\xi(t). \tag{2}$$

The solution-dependent matrix $\mathbf{B}(\mathbf{z})$ takes into account the possible modulation of the noise generators.

The nonlinear perturbation theory in [6] is based on assuming for $\mathbf{z}(t)$ the following decomposition:

$$\mathbf{z}(t) = \mathbf{x}_S(t + \alpha(t)) + \mathbf{y}(t), \tag{3}$$

[1]Departament d'Enginyeria Electrònica, Universitat Autònoma de Barcelona, 08193 Bellaterra (Barcelona), Spain.
[2]Dipartimento di Elettronica, Politecnico di Torino, Corso Duca degli Abruzzi 24, 10129 Torino, Italy. Phone: +39 011 5644140.
Corresponding author:
F. Bonani
Email: fabrizio.bonani@polito.it

where $\boldsymbol{\alpha}(t)$ is a stochastic process responsible for the oscillator phase noise, while $\mathbf{y}(t)$ corresponds to the *orbital fluctuations* (amplitude noise). The autocorrelation matrix of the noisy oscillator solution is therefore given by

$$\begin{aligned}\mathbf{R}_{\mathbf{z},\mathbf{z}}(t,\tau) &= E\{\mathbf{z}(t)\mathbf{z}^{\dagger}(t+\tau)\}\\ &= \mathbf{R}_{\mathbf{x}_S,\mathbf{x}_S}(t,\tau)+\mathbf{R}_{\mathbf{x}_S,\mathbf{y}}(t,\tau)+\mathbf{R}_{\mathbf{y},\mathbf{x}_S}(t,\tau)\\ &\quad+\mathbf{R}_{\mathbf{y},\mathbf{y}}(t,\tau),\end{aligned} \tag{4}$$

where $E\{\cdot\}$ is the ensemble average operator and † denotes the complex conjugate and transpose operation. The first term $\mathbf{R}_{\mathbf{x}_S,\mathbf{x}_S}$ (t, τ) describes phase noise [6].

Notice that the decomposition in (3) was already proposed in [8]: although both [8] and [6] make use of the Floquet theory to develop their analysis, the advantage in the treatment of [6] is in the choice of the projection operator chosen to decompose phase and amplitude fluctuations. Kaertner projects the equation along the tangent vector $\dot{\mathbf{x}}_S(t)=\mathbf{u}_1(t)$, where $\mathbf{u}_1(t)$ is the (direct) Floquet eigenvector associated to the null Floquet exponent $\boldsymbol{\mu}_1=0$ always present when the linear system obtained by linearizing (1) around the steady-state solution $\mathbf{x}_S(t)$ is studied [6, 9]. On the other hand, the derivation in [6] shows that $\boldsymbol{\alpha}(t)$ satisfies a nonlinear stochastic equation, derived by projecting the full equation along the Floquet adjoint eigenvector $\mathbf{v}_1(t)$ associated to $\boldsymbol{\mu}_1$. This decouples $\boldsymbol{\alpha}(t)$ from orbital noise, thus allowing for a separated treatment of the two components.

The proof provided in [7] shows that including orbital fluctuations using the same projection system as in [6], even the total noisy output $\mathbf{z}(t)$ is, at least asympotically with the observation time t, a stationary stochastic process (this result was obtained in [6] with reference to phase noise only, i.e., by setting $\mathbf{y}(t)=0$). This means that, in the frequency domain, a stationary total spectrum can be defined as

$$\mathbf{S}_{\mathbf{z},\mathbf{z}}(\omega)=\mathbf{S}_{\mathbf{x}_S,\mathbf{x}_S}(\omega)+\mathbf{S}_{corr}(\omega)+\mathbf{S}_{\mathbf{y},\mathbf{y}}(\omega), \tag{5}$$

where the partial spectra are the Fourier transforms of the asymptotic values of the correlation functions $\mathbf{R}_{\mathbf{x}_S,\mathbf{x}_S}$, $\mathbf{R}_{\mathbf{x}_S,\mathbf{y}}+\mathbf{R}_{\mathbf{y},\mathbf{x}_S}$ and $\mathbf{R}_{\mathbf{y},\mathbf{y}}$, respectively.

Because of the decoupling of the $\boldsymbol{\alpha}(t)$ equation from $\mathbf{y}(t)$, the phase noise contribution $\mathbf{S}_{\mathbf{x}_S,\mathbf{x}_S}(\omega)$ still is given by the same expression derived in [6]. On the other hand, the second and third term in (5) depend on the remaining $n-1$ Floquet exponents and direct and adjoint eigenvectors associated to the oscillator limit cycle. Closed-form expressions were mathematically derived [7], and reported in [10]. We repeat them here for the sake of self-consistency:

$$\mathbf{S}_{\mathbf{x}_S,\mathbf{x}_S}(\omega)=\sum_h \tilde{\mathbf{X}}_h\,\tilde{\mathbf{X}}_h^{\dagger}\,\frac{h^2\omega_0^2 c}{\Xi_h^2(\omega)} \tag{6}$$

$$\begin{aligned}\mathbf{S}_{corr}(\omega)=\sum_{l=2}^{n}\sum_{h,j}\Bigg\{&\frac{(\mathbf{D}_{lhj}^{\dagger}+\mathbf{D}_{lhj})\left[\tfrac{1}{2}h^2\omega_0^2 c-Re\{\mu_l\}\right]}{\Delta_{lhj}^2(\omega)}\\ &+\frac{i(\mathbf{D}_{lhj}^{\dagger}-\mathbf{D}_{lhj})[\omega+j\omega_0+Im\{\mu_l\}]}{\Delta_{lhj}^2(\omega)}\\ &-\frac{(\mathbf{D}_{lhj}^{\dagger}+\mathbf{D}_{lhj})\left[\tfrac{1}{2}h^2\omega_0^2 c\right]}{\Xi_h^2(\omega)}-\frac{i(\mathbf{D}_{lhj}^{\dagger}-\mathbf{D}_{lhj})[\omega+h\omega_0]}{\Xi_h^2(\omega)}\Bigg\},\end{aligned} \tag{7}$$

$$\begin{aligned}\mathbf{S}_{\mathbf{y},\mathbf{y}}(\omega)=\sum_{l=2}^{n}\sum_{h,j}\Bigg\{&\frac{(\mathbf{C}_{lhj}^{\dagger}+\mathbf{C}_{lhj})\left[\tfrac{1}{2}h^2\omega_0^2 c-Re\{\mu_l\}\right]}{\Delta_{lhj}^2(\omega)}\\ &+\frac{i(\mathbf{C}_{lhj}^{\dagger}-\mathbf{C}_{lhj})(\omega+j\omega_0+Im\{\mu_l\})}{\Delta_{lhj}^2(\omega)}\Bigg\},\end{aligned} \tag{8}$$

where i is the imaginary unit, $\boldsymbol{\omega}_0$ is the angular frequency of oscillation and $\tilde{\mathbf{X}}_h$ is the hth harmonic amplitude of the (exponential) Fourier representation of $\mathbf{x}_S(t)$. The other coefficients are (here $\mathbf{B}^T$ denotes the transpose of $\mathbf{B}$) as follows:

$$c=\frac{1}{T}\int_0^T \mathbf{v}_1^T\mathbf{B}\mathbf{B}^T\mathbf{v}_1\,\mathrm{d}t, \tag{9}$$

$$\Xi_h^2(\omega)=\left[\tfrac{1}{2}h^2\omega_0^2 c\right]^2+[\omega+h\omega_0]^2, \tag{10}$$

$$\Delta_{lhj}^2(\omega)=\left[\tfrac{1}{2}h^2\omega_0^2 c-Re\{\mu_l\}\right]^2+[\omega+j\omega_0+Im\{\mu_l\}]^2, \tag{11}$$

$$\mathbf{C}_{lhj}=\sum_{l'=2}^{n}\sum_{j'}\frac{\tilde{\mathbf{U}}_{l'j'}\,\tilde{\Lambda}_{l'h-j'}^{T}\,\tilde{\Lambda}_{l_{h-j}}^{*}\,\tilde{\mathbf{U}}_{lj}^{\dagger}}{i(j-j')\omega_0-\mu_{l'}-\mu_l^{*}}, \tag{12}$$

$$\mathbf{D}_{lhj}=\tilde{\mathbf{X}}_h\tilde{\mathbf{V}}_{1_0}^{T}\,\tilde{\Lambda}_{l_{h-j}}^{*}\,\tilde{\mathbf{U}}_{lj}^{\dagger}\frac{ih\omega_0}{-\mu_l^{*}-i(h-j)\omega_0}. \tag{13}$$

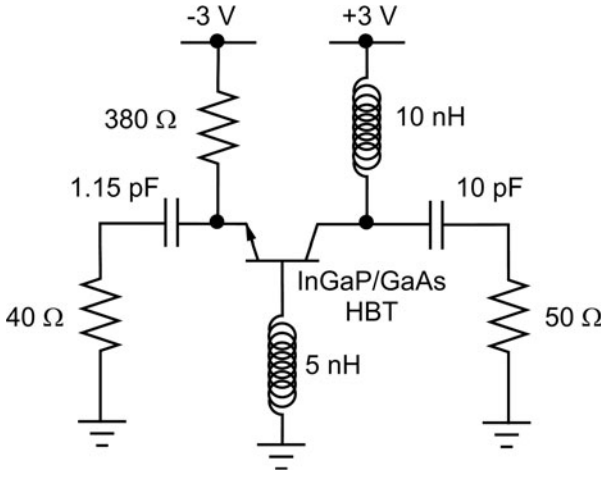

Fig. 1. Circuit of the InGaP/GaAs HBT oscillator in [15].

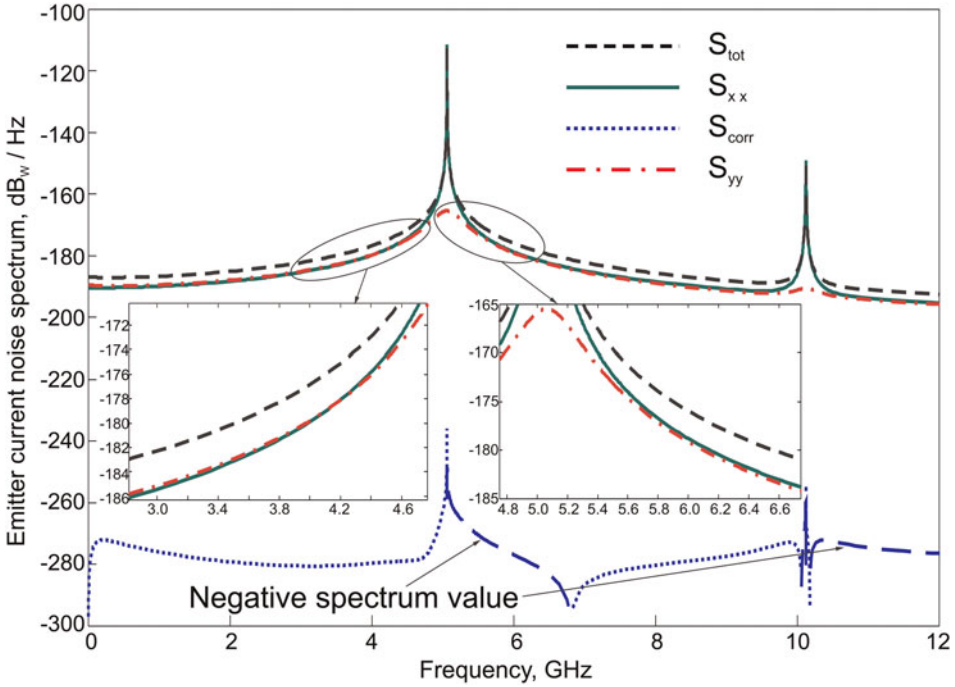

Fig. 2. Total emitter current noise spectrum of the InGaP/GaAs HBT oscillator as a function of the absolute frequency (from [10]).

In the previous expressions $\tilde{\mathbf{V}}_{1_o}$ is the DC harmonic component of $\mathbf{v}_1(t)^T\mathbf{B}(t)$, and $\tilde{\mathbf{U}}_{l_j}$ and $\tilde{\Lambda}^T_{l_k}$ are the Fourier coefficients of $\mathbf{u}_l(t)$ and $\mathbf{v}_1^T(t)\mathbf{B}(t)$, respectively.

Accordingly, the full noise spectrum evaluation is straightforward once two deterministic analyses are performed:

1. the oscillator working point $\mathbf{x}_S(t)$ is calculated in the time or frequency domain, along with the oscillation frequency;
2. the oscillator equations are linearized around the limit cycle $\mathbf{x}_S(t)$, and the corresponding linear system is analyzed according to the Floquet theory estimating all the n Floquet exponents μ_l, and all the associated direct $\mathbf{u}_l(t)$ and adjoint $\mathbf{v}_l(t)$ Floquet eigenvectors ($l = 1, \ldots, n$). This evaluation can be, for instance, carried out in the frequency domain with the algorithms in [9, 11].

III. RESULTS AND DISCUSSION

We consider here two examples of application: the HBT oscillator discussed in [10] and the Tow-Thomas oscillator studied in [6, 12, 13]. All simulations are carried out exploiting a simulation code written in the MATLAB environment [14].

Table 1. Floquet's exponents for the HBT oscillator.

Exponent	Value [s^{-1}]
μ_1	0
μ_2	-1.27×10^9
μ_3	$-2.50 \times 10^9 + i1.94 \times 10^9$
μ_4	$-2.50 \times 10^9 - i1.94 \times 10^9$
μ_5	-1.14×10^{10}
μ_6	-4.71×10^{11}

A) HBT-based oscillator

The first example is the negative-resistance oscillator shown in Fig. 1 [15]. The active device is an InGaP/GaAs HBT represented by the Gummel-Poon model described in [15], made of a static model complemented by the nonlinear capacitances connected between the base and emitter, and the base and collector. The emitter of the circuit exhibits a negative resistance and the rest of the circuit was designed to set up oscillations at 5 GHz. The circuit was simulated in the frequency domain with the harmonic balance (HB) technique including 30 harmonics plus DC. The calculated total emitter current noise spectrum and its components according to (5) are shown in Fig. 2 as a function of the absolute frequency. We found that the correlation spectrum is negligible, while orbital noise becomes the dominant term for frequencies away from the harmonics. The circuit is represented by

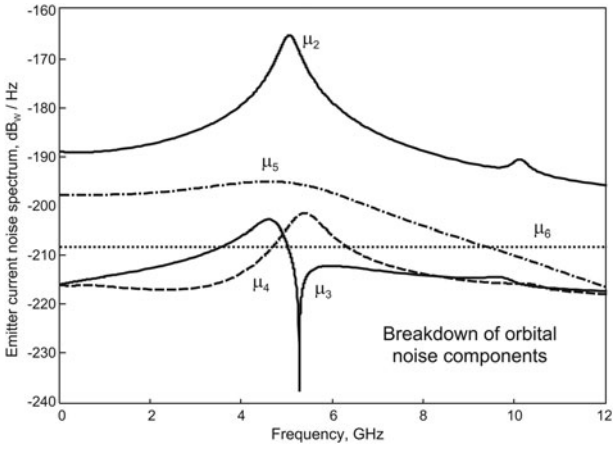

Fig. 3. Partial contributions to the orbital emitter current noise spectrum of the InGaP/GaAs HBT oscillator (from [10]).

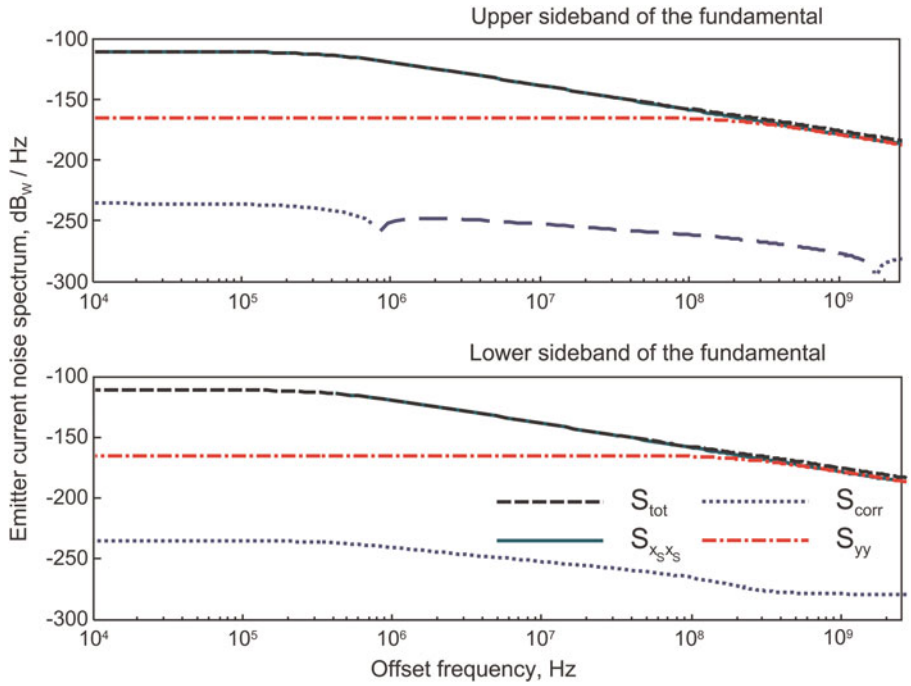

Fig. 4. Upper and lower sideband total emitter current noise spectrum of the InGaP/GaAs HBT oscillator around the fundamental (from [10]).

a differential algebraic equation system made of nine scalar equations: according to [16], there are three infinite Floquet exponents and six Floquet exponents with the finite values listed in Table 1: apart from μ_1, all exponents have negative real part thus implying that the oscillator is stable.

According to the expressions in [7, 10], the partial contributions to the orbital noise spectrum due to the five non-null Floquet exponents are reported in Fig. 3. The dominant contribution is due to the exponent with the smallest real part, in qualitative agreement with the fact that the lth Floquet eigenvalue contribution to $\mathbf{S}_{y,y}(\boldsymbol{\omega})$ is proportional to $1/\boldsymbol{\mu}_l$ [10]. Notice, however, that the second largest component is due to $\boldsymbol{\mu}_5$, thus pointing out that the magnitude of the Floquet exponents is not the only contribution to be taken into account to assess the relative importance of amplitude noise.

Figs 4 and 5 show, respectively, the sideband representation of the noise spectrum around the fundamental and the second harmonic component: the orbital contributions result into

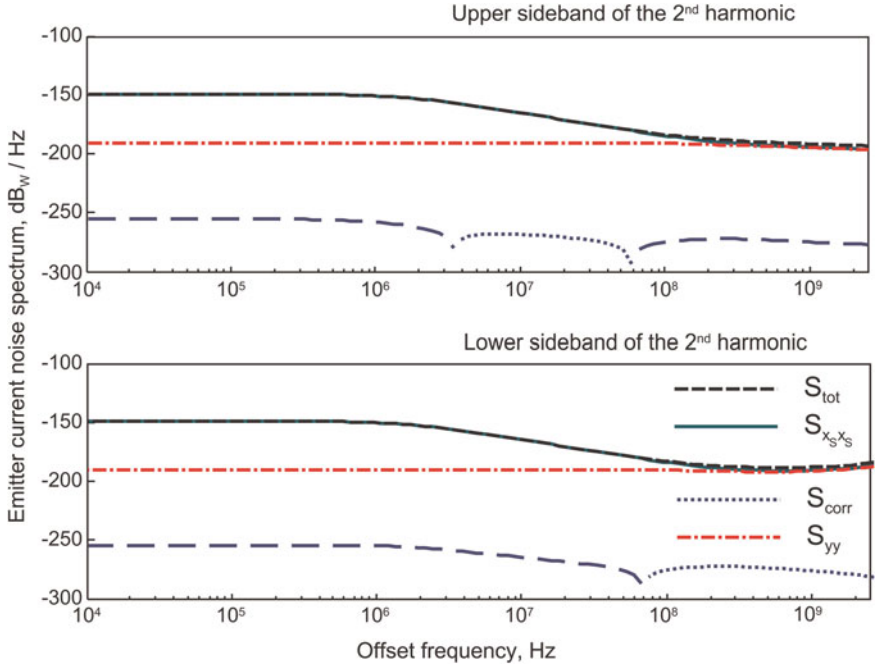

Fig. 5. Upper and lower sideband total emitter current noise spectrum of the InGaP/GaAs HBT oscillator around the second harmonic (from [10]).

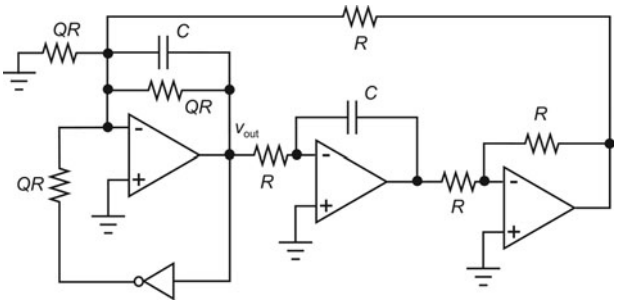

Fig. 6. Circuit of the Tow-Thomas oscillator. We used $R = 1\ \mathrm{k}\Omega$ and $C = 20$ nF.

asymmetries in the spectrum around the oscillator harmonics, as also found in [17].

B) Tow-Thomas oscillator

The second example is the Tow-Thomas oscillator presented in [6, 12, 13] and shown in Fig. 6. The operational amplifiers are ideal, noiseless and represented by nullors, while the inverter is approximated by the input–output relation $v_{out} = \tanh(-\alpha v_{in})$, where $\boldsymbol{\alpha}$ is a parameter representing the slope of the transition. This circuit was chosen since it can be shown to be equivalent [6] to a parallel *RLC* circuit with a *Q* factor corresponding to the *Q* coefficient in Fig. 6: this allows for a simple modulation of the *Q* value to study its impact on orbital noise. The output variable chosen for noise estimation is voltage v_{out}.

The oscillator has two state variables, therefore only two Floquet exponents $\boldsymbol{\mu_1} = 0$ and $\boldsymbol{\mu_2}$ are present. The circuit was simulated with HB including 50 harmonics plus DC, assuming $\boldsymbol{\alpha} = -3$ and considering as noise sources only the thermal noise in the resistances. The resulting oscillation frequency is $f_o = 7.9172$ kHz, while the *Q*-dependence of $\boldsymbol{\mu_2}$ (a real, negative number as expected for a stable oscillator) is presented in Fig. 7: as discussed in [16], a high-*Q* oscillator is characterized by at least a second Floquet exponent near to zero, which in turn should result into a larger amplitude noise component.

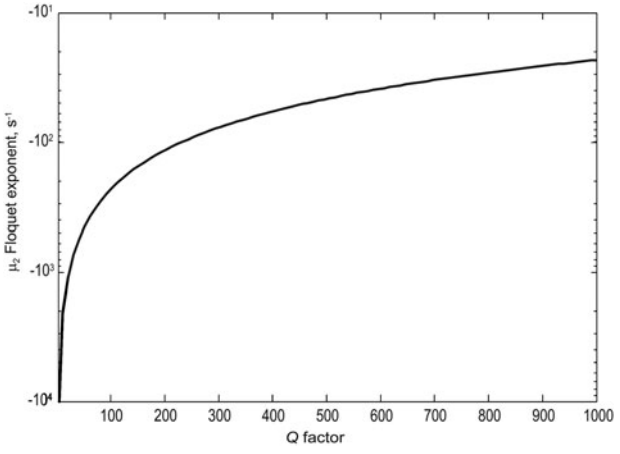

Fig. 7. Floquet exponent $\boldsymbol{\mu_2}$ for the Tow-Thomas oscillator as a function of the *Q* factor of the equivalent *RLC* circuit.

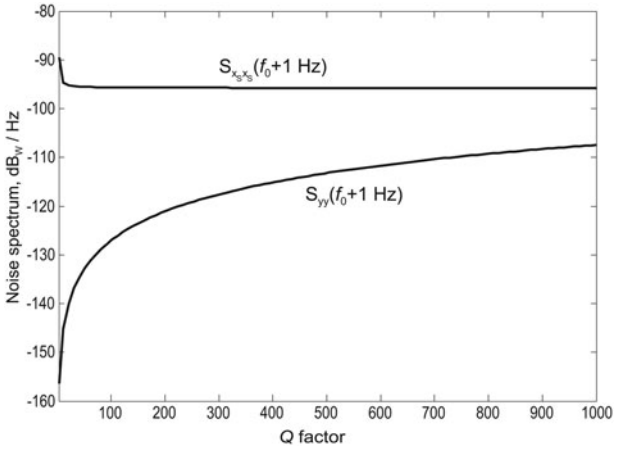

Fig. 8. *Q*-dependence of the phase and amplitude noise spectra at 1 Hz offset frequency from f_o for the Tow-Thomas oscillator.

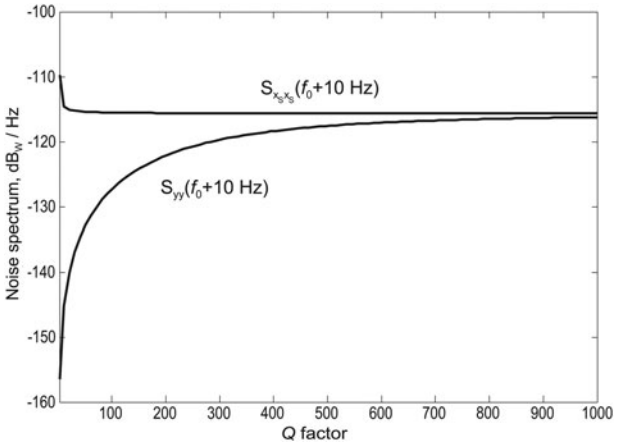

Fig. 9. *Q*-dependence of the phase and amplitude noise spectra at 10 Hz offset frequency from f_o for the Tow-Thomas oscillator.

This is confirmed by Figs 8–10, which report the *Q*-dependence of the phase and orbital noise spectra at an offset frequency of 1, 10 and 100Hz from f_o, respectively. As expected, the amplitude noise is steadily increasing with

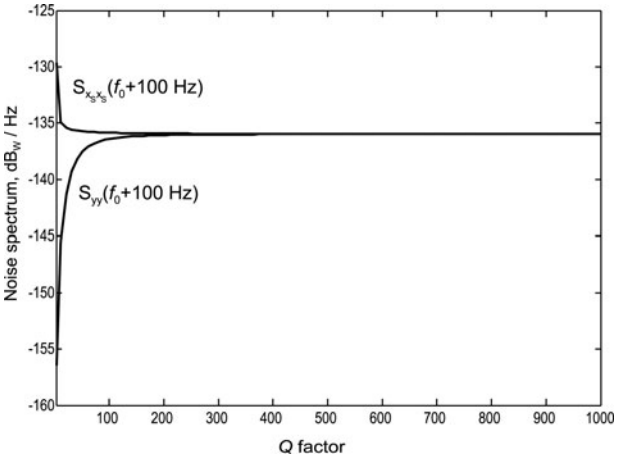

Fig. 10. *Q*-dependence of the phase and amplitude noise spectra at 100 Hz offset frequency from f_o for the Tow-Thomas oscillator.

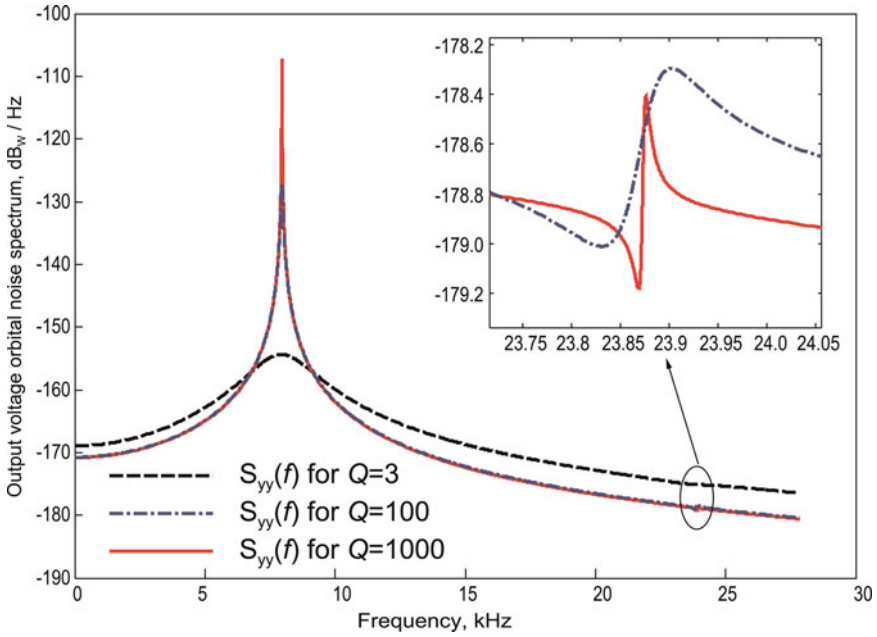

Fig. 11. Orbital noise spectrum of the Tow-Thomas oscillator as a function of the absolute frequency for three values of Q.

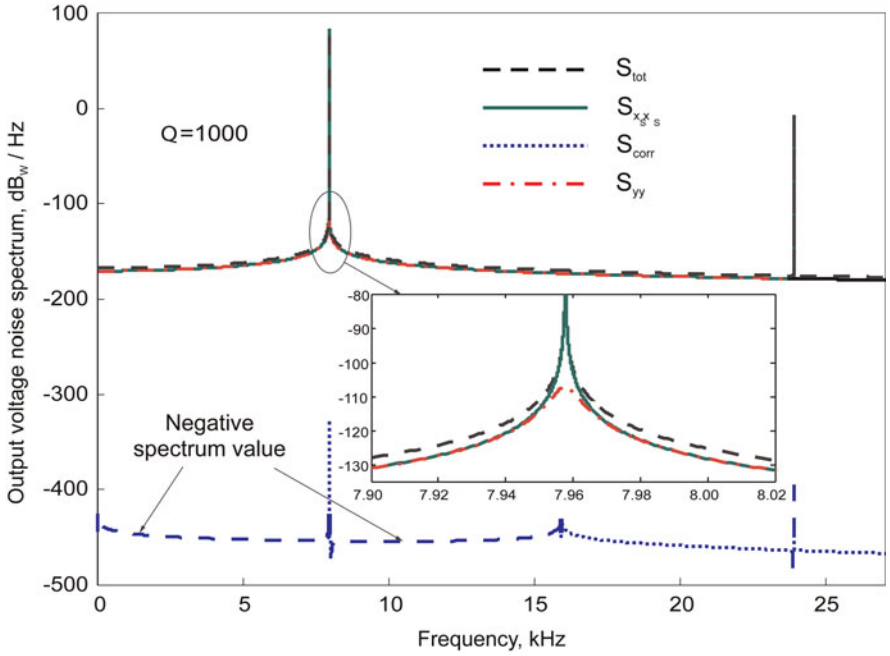

Fig. 12. Total noise spectrum of the Tow-Thomas oscillator as a function of the absolute frequency for $Q = 1000$.

Q, reaching a maximum value equal to the corresponding phase noise spectrum. The absolute frequency dependence of the orbital noise spectrum using Q as a parameter is presented in Fig. 11, again confirming the impact of Q on the magnitude of amplitude noise. Notice also that in this circuit the correlation between phase and orbital fluctuations is negligible, as shown in Fig. 12, where the total output voltage noise spectrum and its partial components are shown for $Q = 1000$ as a function of the absolute frequency. Spectrum peaks are present at f_o and $3f_o$ only, as found also in [6, 12].

Finally, we show the offset frequency dependence of the relevant noise contributions around the fundamental and third harmonics in Figs 13 and 14, respectively. For this oscillator, although the noise spectrum is practically symmetric around the fundamental, an asymmetry appears around the third harmonics, again due to the orbital noise contribution.

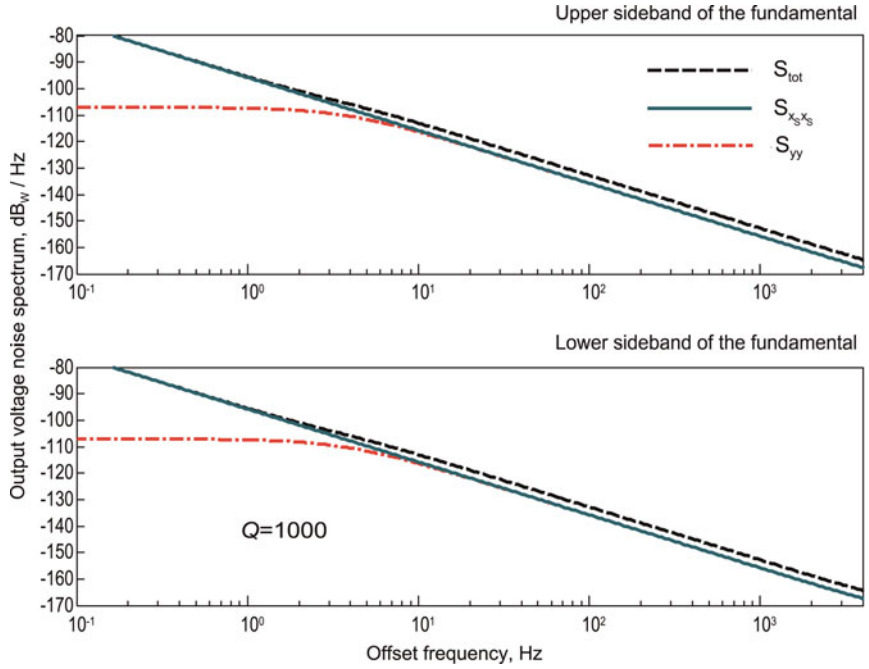

Fig. 13. Upper and lower sideband total noise spectrum of the Tow-Thomas oscillator around the fundamental for $Q = 1000$.

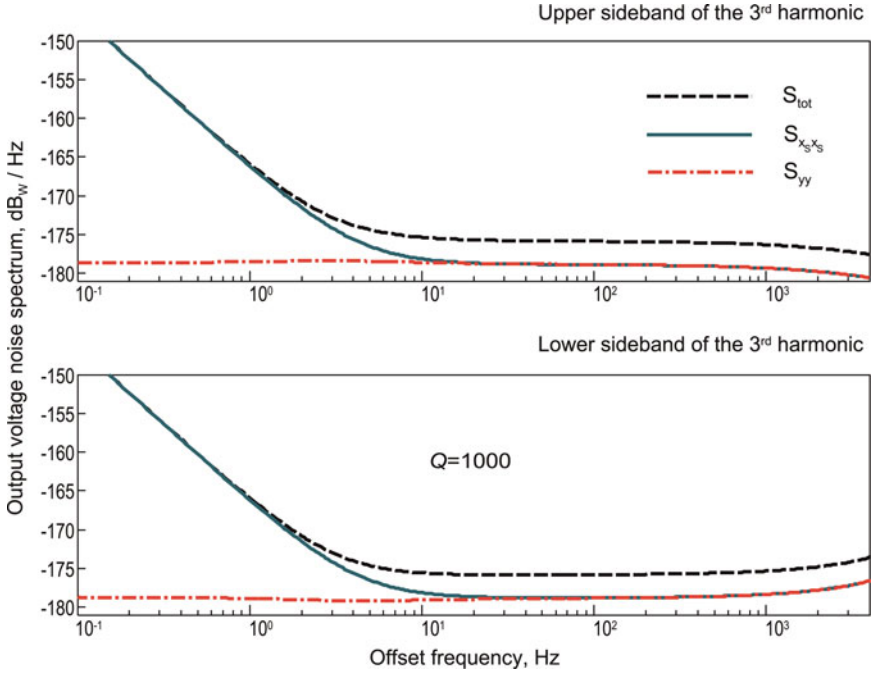

Fig. 14. Upper and lower sideband total noise spectrum of the Tow-Thomas oscillator around the third harmonic for $Q = 1000$.

VI. CONCLUSION

Based on the rigorous extension of the nonlinear perturbative approach to oscillator noise analysis proposed in [6], we discussed the effects of orbital noise on the fluctuation spectrum of autonomous circuits. We have provided two examples of application, showing that amplitude noise, the dominant fluctuation component sufficiently far away from the oscillation frequency, might be responsible for spectrum asymmetries around the oscillation frequency harmonics. Furthermore, we have provided evidence that orbital noise actually becomes more significant for high-Q oscillators, since its magnitude is, at least for the second-order oscillator considered in this study, an increasing function of the Q factor.

ACKNOWLEDGEMENTS

We acknowledge the partial support of Regione Piemonte through the research project CNT4SIC, and of the Spanish

MEC project TEC 2009-06986. We also thank Dr. Simona Donati Guerrieri and Dr. Federica Cappelluti of Politecnico di Torino for useful discussions.

REFERENCES

[1] Berstein, I.L.: On fluctuations in the neighborhood of periodic motion of an auto-oscillating system. Doklad. Akad. Nauk., **20** (1938), 11.

[2] Hafner, E.: The effect of noise in oscillators. Proc. IEEE, **54** (1966), 179–198.

[3] Lax, M.: Classical noise. V. Noise in self-sustained oscillators. Phys. Rev., **160** (1967), 290–306.

[4] Kurokawa, K.: Noise in synchronized oscillators. IEEE Trans. Microw. Theory Tech., **16** (1968), 234–240.

[5] Hajimiri, A.; Lee, T.H.: The Design of Low Noise Oscillators, Kluwer Academic Publishers, Dordrect, 1999.

[6] Demir, A.; Mehrotra, A.; Roychowdhury, J.: Phase noise in oscillators: a unifying theory and numerical methods for characterization. IEEE Trans. Circ. Syst. I: Fund. Theory and Appl., **47** (2000), 655–674.

[7] Traversa, F.L.; Bonani, F.: Oscillator noise: a nonlinear perturbative theory including orbital fluctuations and phase-orbital correlation. IEEE Trans. Circ. Syst. I: Regular Papers (2011), submitted.

[8] Kaertner, F.X.: Determination of the correlation spectrum of oscillators with low noise. IEEE Trans. Microw. Theory Tech., **37** (1989), 90–101.

[9] Traversa, F.L.; Bonani, F.; Donati Guerrieri, S.: A frequency-domain approach to the analysis of stability and bifurcations in nonlinear systems described by differential-algebraic equations. Int. J. Circuit Theory Appl., **36** (2008), 421–439.

[10] Traversa, F.L.; Bonani, F.: Oscillator noise: a rigorous analysis including orbital fluctuations. Workshop on Integrated Nonlinear Microwave and Millimetre-wave Circuits (INMMIC), Göteborg, Sweden, 2010.

[11] Traversa, F.L.; Bonani, F.: Frequency domain evaluation of the adjoint Floquet eigenvectors for oscillator noise characterization. IET Circuits, Devices Syst. (DOI: 10.1049/iet-cds.2010.0138), (2011), to appear

[12] Dec, A.; Toth, L.; Suyama, K.: Noise analysis of a class of oscillators. IEEE Trans. Circuits Syst., **45** (1998), 757–760.

[13] Brambilla, A.; Gruosso, G.; and Storti Gajani, G.: Determination of Floquet exponents for small-signal analysis of nonlinear periodic circuits. IEEE Trans. Computer-Aided Design Integr. Circuits Syst., **28** (2009), 447–451.

[14] MATLAB, The Mathworks, Natick, MA, USA. www.matlab.com

[15] Sweet, A.A.: Designing Bipolar Transistor Radio Frequency Integrated Circuits, Artech House, Norwood, 2008.

[16] Demir, A.: Floquet theory and non-linear perturbation analysis for oscillators with differential-algebraic equations. Int. J. Circ. Theory Appl., **28** (2000), 163–185.

[17] Brambilla, A.; Gruosso, G.; Redaelli, M.A.; Storti Gajani, G.; Caviglia, D.D.: Improved small signal analysis for circuits working in periodic steady state. IEEE Trans. Circ. Syst. I: Regular Papers, **57** (2010), 427–437.

Fabio L. Traversa was born in Bari, Italy, in 1979. He received the Laurea degree in Nuclear Engineering, and the Ph.D. degree in Physics from Politecnico di Torino, Italy, in 2004 and 2008, respectively. During 2008, he was a researcher fellow with the Electronics Department of the same institution, and since 2009 he is a Postdoctoral researcher at the Departament d'Enginyeria Electrònica, Universitat Autònoma de Barcelona, Spain. His research interests are mainly devoted to the physics-based simulation of transport in nano-devices, with special emphasis on the analysis and simulation of quantum correlations. Furthermore, he is also interested in the stability analysis of nonlinear circuits and systems, and in the noise analysis of nonlinear circuits.

Fabrizio Bonani was born in Torino, Italy, in 1967. He received the Laurea degree, *cum laude*, and the Ph.D. degree in Electronic Engineering from Politecnico di Torino, Italy, in 1992 and 1996, respectively. Since 1995, he has been with the Electronics Department of the same institution, where he currently is an Associate Professor of Electronics. His research interests are mainly devoted to the physics-based simulation of semicondutor devices, with special emphasis on the noise analysis of field-effect and bipolar transistors, to the thermal analysis of power devices and circuits, and to the simulation and design of power semiconductor devices. He is also interested in the stability analysis of nonlinear circuits and systems, and in the noise analysis of nonlinear circuits.

From October 94 to June 95 he has been with the ULSI Technology Research Department of Bell Laboratories in Murray Hill (NJ) as a consultant, working on physics-based noise modeling of electron devices. From August to October 2008, he was Visiting Scientist at the Ferdinand-Braun-Institut für Höchstfrequenztechnik, Berlin, Germany, developing compact noise models for linear and nonlinear applications. He is a Senior Member of IEEE, and a member of the MTT-14 Technical Committee on Low-Noise Techniques. Since 2010, he serves in the Modeling and Simulation committee of IEDM.